

Encapsulation for long-term stability enhancement of perovskite solar cells

Fabio Matteocci¹, Lucio Cinà¹, Enrico Lamanna¹ Stefania Cacovich², Giorgio Divitini², Paul A. Midgley², Caterina Ducati² and Aldo Di Carlo^{1,*}

1. *C.H.O.S.E. (Centre for Hybrid and Organic Solar Energy), Department of Electronic Engineering, University of Rome "Tor Vergata", via del Politecnico 1, Rome 00133, Italy*

2. *Department of Materials Science & Metallurgy, University of Cambridge, 27 Charles Babbage road, CB3 0FS, Cambridge, UK*

* *Email: aldo.dicarlo@uniroma2.it*

Keywords: perovskite solar cell, encapsulation, sealing process, stability, large area

Abstract

Perovskite Solar Cells (PSCs) have achieved power conversion efficiencies (PCEs) comparable to established technologies, but their stability in real-life working conditions – including exposure to moisture, heat and light - has still not been decisively demonstrated. Encapsulation of the cells is vital for increasing device lifetime, as well as shedding light on the intrinsic degradation process of the active layers. Here we compare different sealing protocols applied to large area cells (1 cm², average PCE 13.6%) to separate the extrinsic degradation, due to the external environment, from the intrinsic one, due to the materials themselves. Sealing methods were tested against accelerated life-time tests – damp-heating, prolonged heating and light-soaking. We thus developed and tested a novel sealing procedure that makes PSCs able to maintain a stabilized 10% PCE after heat, light and moisture stress.

1. Introduction

Together with efficiency and cost, the stability is one of the crucial factors to validate photovoltaic (PV) technologies [1, 2]. Perovskite solar cells (PSCs) represent a promising PV technology due to the high power conversion efficiency (PCE) already reached in few years of intensive research [3] and the cost-effective materials and fabrication process [4-10]. Nevertheless, PSC stability is still a major issue which need to be solved for an effective industrial exploitation.

Measurement protocols focusing on the solar cell stability have been identified for conventional (IEC standards [11]) and organic (ISOS standards [12]) PV technologies. Although, there is not yet a specific stability protocol for PSCs, stability studies have been recently performed [13-16] and several key elements were identified as impacting the stability of PSCs. [17-19] The degradation mechanisms are mainly related to oxygen and moisture (environmental stability), [15, 20, 21] temperature and intrinsic heating under applied voltage (thermal stability) [22-24] and light (photo-stability). [25-28]

The aim of the paper is the investigation of robust and cost-effective sealing procedures to stabilize the PSC devices under several Accelerated Life Time (ALT) tests, such as damp-heat, light-soaking and temperature stress. Both intrinsic stability (related to the constituent materials and dopants) and the extrinsic stability (affected by the sealing procedure) will be discussed.

Environmental stability studies have mainly focused on the degradation of PSCs induced by moisture, which can rapidly degrade the organometal halide perovskites. In particular, methylammonium (MA) lead triiodide (MAPbI_3) perovskite immediately decomposes into MA, HI and PbI_2 in a wet environment due to its solubility in water. [21] The insertion of bromine atoms in the perovskite structure ($\text{MAPbBr}_x\text{I}_{3-x}$) can increase the environmental stability, as reported by Noh et al. [20] The moisture induced degradation can be reduced by optimizing the constituent materials, [29-34], the architecture of the cell [25, 35-38], the interfaces [27, 39-42] and the environment conditions during the fabrication steps [43, 44]. In particular, the use of carbon-based materials as Hole Transporting Layer (HTL) and back-contact can protect the perovskite layer from moisture infiltration due to its highly hydrophobic nature [13, 16, 45]. In the literature, moisture resistance is

usually evaluated using shelf life tests of non-encapsulated cells. Sealing of the cell is, however, a requirement for the device normal operation and should be considered to assess the stability of the cell [46, 47].

The thermal stability is assessed analyzing material, interfaces and sealing properties under heating and cooling cycles. Early degradation of PSCs induced by thermal cycling has been investigated by Divitini et al. [22] combining TEM and electrical characterization, finding a reversible behavior of cell performance under thermal cycles between 20 °C and 90 °C and no chemical/morphological changes of the perovskite layer until 150°C. At higher temperature, TEM analyses shows a clear lead and iodine migration toward the device interfaces. A superior thermal stability was showed by Sutton et al using fully inorganic perovskite structure (CsPbI₂Br) with a stabilized efficiency of 5.6%. The results show that the replacement of the organic cation (MABr) with a inorganic one (CsBr) prevents the thermal induced degradation at 85°C for 250 hours as confirmed through UV-Vis absorbance and X-Ray Diffraction (XRD) spectra [48]. The thermal stability is also influenced by the temperature dependence of the electrical properties of Spiro-OMeTAD as showed by Malinauskas et al. for solid-state dye sensitized solar cell. The results show a temperature (60°C) induced formation of large Spiro-OMeTAD crystalline domains leading to a decrease of PV performance (-60%) after 120hours [49]. Light stability of PSCs, i.e. the effect of the light exposure on the optical/electric properties of the cell, has been investigated by several authors and has been addressed as the main stability issue of PSCs [11, 12]. It is known that UV light induces the degradation of the mesoscopic TiO₂-based PSC devices due to trap-assisted recombinations. Leijtens et al. proposed that the UV-aged cells suffer from a deep trapping of injected electrons within available sites in the TiO₂ [25]. Then, a decrease in the short-circuit current J_{SC} is showed due to the charge recombination with oxidized Spiro-OMeTAD species on the μ s-ms time-scale as proven using transient absorption spectroscopy. This degradation mechanism was showed for both mesoporous/planar TiO₂ devices indicating that the light induced trap sites in the TiO₂ constitute a rapid degradation pathway for photo-generated electrons, leading to lower charge collection

efficiency. Although the use of UV filters could suppress the UV-induced degradation, further optimization of the ETL materials and ETL/Perovskite interface is required. Li et al. show that CsBr used as interfacial modifier on the surface of the TiO₂ ETL delays the UV-induced degradation of the TiO₂-based PSC devices due to the reduced chemical reactivity of TiO₂ and the reduced defect density at the perovskite/TiO₂ interface [50].

Organometal trihalide perovskite also shows photo-instability under light exposure in the visible wavelengths (LED lamp) when the stability test are performed in air. Bryant et al. show rapid decrease of the PV performance under continuous illumination in dry air of unsealed MAPbI₃-based PSC (80% relative decrease after 4h), while a negligible PCE decrease was observed in a nitrogen-filled box (around 5% relative decrease after 4h) [51]. The author claims that the presence of oxygen acts as main degradation factor during the light stability test: oxygen induces the formation of deep trap sites in the compact and mesoporous TiO₂ layers as previously showed for UV-induced degradation. Photo-induced degradation was also reported from Wei et al. showing the detrimental effect of the continuous light exposure using both planar and mesoscopic architectures [27]. The PCE values of planar PSCs decreased from 18% to 2.4 % after 180 minutes of exposure time. This rapid decrease is related to the light soaking that leads to insufficient hole extraction at HTL/Au electrode interface. Interestingly, the re-deposition of the Au electrode on degraded devices causes a remarkable recovery of the PV performance, of around 80% for both PSC architectures. Sanhira et al. show that the use of MoO_x (15nm) as interlayer between Spiro and the metal electrodes increases the light stability of PSC devices. In fact, a planar PSC device using 15nm-thick MoO_x/Al electrode shows lower PCE decrease (-60% with respect to the initial value) with respect to an Al electrode after 120h of light soaking [52]. Several authors also considered the combined action of light-soaking and temperature. Bush et al. show the effect of the low/high temperature (35°C and 100°C, respectively) on the stability of semi-transparent and opaque PSC during a light soaking test at Maximum Power Point (MPP) for perovskite/silicon tandem solar cell. Interestingly, the semi-transparent cell shows a T₈₀ lifetime (defined as the time where the PCE measured under stability

test is 80% of the initial value) of 124h at 100°C without additional sealing. The sputtered ITO back-contact shows better light, thermal and environment stability than the opaque ZnO/Al/Ag backcontact. At the same stress conditions, extremely fast degradation of the opaque cells ($T_{80} \sim 0.1$ hour) was correlated to the metal corrosion induced by the degradation of the perovskite layer at high temperature [53].

Katz et al. reports the induced degradation of MAPbX₃ (I,Br) films, not packaged in devices, by exposure to concentrated sunlight of 100 Sun at relatively high temperature (45-55°C). The study shows the superior light/thermal stability of MAPbBr₃ perovskite, where no photo-bleaching was observed after 1 hour. The author claims that the light and thermal induced degradation mechanisms are highly correlated to the perovskite structure [54].

Recently, Domanski et al. reported a further process for the thermal induced degradation. A light/thermal stress was performed at 75°C under a white LED source using a MPP tracker. On a short timescale (12hours), the author claims that degradation is caused by the electrode migration on the perovskite film (50% relative decrease after 12hour using an unsealed device) [55].

These works have clarified some specific effects influencing stability of PSCs, but it was not always possible to distinguish between degradation induced by intrinsic stability of the materials and interfaces and degradation influenced by the poor encapsulation conditions (when used). Moreover, each of the works mentioned above was describing a particular ALT test without comparing, on the same PSCs batch, all the three main ALT test, namely light-soaking, damp-heat and temperature stress. The scope of the present work is to fill this gap and to report on the development of an optimized encapsulation strategy and on a comprehensive study of intrinsic PSCs stability assessed using the three main ALT tests.

2. Results and Discussion

Large area (1.05 cm², Fig. 1a) PSCs are fabricated using a solvent engineering method [56] (see SI). The PCE dispersion graphs of the entire PSC set (23 cells) measured in reverse scan, forward scan and 180s-long MPP tracking are reported in Fig. 1b (average photovoltaic parameters are in Table S1). As expected, the results show that the PCE values extracted at the MPP condition are lower than the same under reverse scan where the current is slightly overestimated by the capacitive effect on the cell [57, 58]. This is confirmed comparing the J_{SC} values under forward and reverse scan with respect to the J_{MPP} values extracted from the MPP tracking (Fig. S1).

After the initial characterization, PSCs are glass-glass encapsulated using several sealing procedures (SPs), varying sealing material and curing strategies as described in the experimental section and schematically reported in Tab.1. Encapsulated cells are tested under stress conditions as reported in the following.

2.1 Shelf-life Test

The impact of the sealing procedure (SP-A, SP-B, SP-C and SP-D) on the performance of the cells is evaluated comparing the PCE values prior ($t=0h$) and after the sealing process, considering a stabilization time (dark and 30% RH) of 20h as reported in Tab. 1. SP-A (Surlyn 60) shows a remarkable decrease of the PCE value (-32.4%) due mainly to the decrease of the current density (-16.4%) and the FF values (-13.7%). A similar impact of this sealing procedure is also observed by Burschka et al. where a PCE decreased from 12.5% (unsealed PSC) to 8.2% (PSC sealed with Surlyn) was reported [59]. This is mainly due to the heating of the cell at the curing temperature (100°C) of the thermo-plastic sealant. In fact, a PCE decrease of only -7.6% is obtained when the cell is sealed at room temperature applying a pressure of 0.4 bar.

SP-B (UV-curable glue deposited on whole active area) shows a lower PCE decrease (-18%) with respect to SP-A. No visible chemical reaction between glue and the active materials is noted using a fresh batch of glue. The PCE decreases could be related both to the UV light exposure and to the UV-induced heating. In fact, the UV illumination could rapidly degrade the TiO₂-based perovskite

solar cell due to trap-assisted recombination of the photo-generated electrons in the TiO₂ [25]. To evaluate the contribution of the UV-induced heating (up to 70°C for a light soaking of 40 s) to the PCE degradation, the UV curable-glue is deposited on the edge of the protective glass only. Then, the active area is masked to avoid the UV light exposure during the curing process. In this way, the sealed device shows only a PCE reduction of 10% with respect to the initial value. Thus we can conclude that both UV light exposure and UV-induced heating contribute almost with the same weight to the degradation of PSCs sealed with SP-B.

SP-C sealing determined a similar decrease of the photovoltaic performance (14.3%). In this case, the glass-glass methacrylate glue (Henkel) is cured upon light exposure using a Xenon lamp at 1Sun intensity for 10s. The decrease could be related to the reaction of the active layers with vapors outgassing from the glue during the light-assisted curing as previously reported from Han et al.[14]. To prevent chemical components of the glue affecting the active layers, Kapton polyimide adhesive is used as first step in the SP-D before gluing glass-to-glass as realized in SP-C. Kapton is commonly used for electronic and photovoltaic applications due to the excellent properties in terms of its chemical/temperature resistance [60, 61]. The Kapton film is covered with a silicon-based adhesive to permit the lamination of the perovskite solar cell over the whole active area. The reduction of PCE for SP-D after 20h from the sealing is only 4% of the PCE before sealing. SP-D sealing is the only approach that resulted in a lower degradation, after 20h, than the unsealed device. To confirm this point, we measured the PCE prior and after SP-D sealing process on the batch with 23 PSCs of Fig.1b. The results show that SP-D has a minimal effect (-1.5%) on the PCE of the cells (Fig.S2).

For all the sealing procedures, shelf-life test continued for 170 hours (Fig. 1c). The degradation of the unsealed PSCs, as well as SP-A, SP-B and SP-C, is very significant, ranging from -58% of SP-A to -22.5% of SP-B and SP-C. On the contrary, SP-D preserved cell performance over the 170 hours.

A shelf-life test of 1500 hours under dark and low humidity condition (30% RH) is performed using a batch of six large area PSCs sealed with SP-D (Fig. 1d). The initial PCE value is referred to the first IV measurement after the sealing procedure. The results show slightly higher PCE after 1350h with respect to the initial PCE (+3%) but 10% lower with respect to the maximum obtained after 100h as reported in Fig. 1d.

2.2 Damp-Heat Test

Due to the superior sealing properties, SP-D is used for a damp-heat test (humidity test) with a temperature in the range 40-50°C and 95% Relative Humidity (RH). Lateral degradation due to the permeation of the water vapors from the edges is one of the critical issues for such test [62, 63]. To increase the moisture resistance of SP-D, a sealant (Threebond glue) is deposited on the edge between the FTO and the protective glass and UV cured for 40s. The active area of the cell is protected during UV irradiation with a black adhesive. We refer to this improved sealing procedure as SP-DES . The damp-heat test is performed on five devices (three SP-DES, one SP-D cell and one unsealed cell). The results of the test is reported in Fig. 2a, together with pictures of stressed devices (Fig. 2b) before and after the 104 hours test. As expected, the color of the unsealed device turns from dark brown to yellow after a few minutes of the damp-heat test. After 7 hours, the unsealed cell shows a completed hydration of the perovskite layer and only a light pink color is left due to the oxidation of the Spiro-OMeTAD layer. The cell with SP-D shows a remarkable PCE decrease in the first 32h (-30%) but not related to the lateral degradation of the perovskite layer. From 32h to 104h, the PCE shows a strong decrease (-95%) related to the moisture-induced degradation of the perovskite layer due to the sealing failure at the glass edges. This is clearly showed in the front side image of PSC with SP-D in Fig. 2b, where the perovskite turned from black/brown to yellow. PSCs sealed with SP-DES show a less pronounced PCE decrease with respect to SP-D in the first 32h (-22%) that further reduces to only -5% from 32h to 102h. Cells with SP-DES do not show any lateral

degradation as confirmed by the front-side image of the PSC, which remains black/brown also after 104 h of damp-heat. This proves the effectiveness of the edge sealant as moisture barrier. The PCE reduction observed in the first few hours for PSCs sealed with SP-DES is not related to moisture but to the temperature stress, as discussed in the following.

2.3 Thermal Test

In order to study the intrinsic effect of the temperature on the PSCs performance, a 250h-long thermal test is performed at 60°C (from 0 to 124h) and 85°C (from 124h to 250h). A batch of six PSCs with SP-DES are stressed in an oven in dark with a relative humidity level of 25 RH% (dry-heat). The normalized average PCE value is reported in Fig.3a.

An early PCE degradation (-7% of the value before heating), is observed after 5h at 60°C mainly due to the decrease of the V_{OC} (Fig. 3a) and FF (Fig. 3c). From 5h to 124h, the normalized PCE shows a linear decrease with a slope of -0.1%/hour mainly induced by the FF decrease. The reduction of FF is due to the increase of the series resistance of the cell under thermal stress (see Fig.S3a-b). According to our previous TEM investigation, the $CH_3NH_3PbI_3$ perovskite composition is not changing during the thermal stress at 60°C [22]. This is also confirmed by the negligible decrease of the J_{SC} value (less than 1%) in the first 124h. Increasing the stress temperature up to 85°C the PCE reduction slope increases to 0.21%/hour. In this case the main responsible are the reduction in FF and J_{SC} . We can associate this PCE decrease to the intrinsic thermal instability of the Spiro-OMeTAD layer. It has been already reported that the transport properties of Spiro-OMeTAD are affected when the film is heated at 60°C due to the partial transformation from amorphous to crystalline phase[49]. To demonstrate the detrimental effect of the temperature on the doped-Spiro-OMeTAD layer, the rectifying behavior of FTO/doped Spiro-OMeTAD/Au diode-like device is assessed under thermal stress (60°C) for 234 hours. We observe an enormous increase of the diode forward resistance up to +80% after 172 h of thermal stress (see SI, Fig. S4). This clearly indicated that the temperature affected the transport properties of the Spiro-OMeTAD HTL. Furthermore, the electrode migration is another detrimental factor referred to the thermal test. We

clearly see this effect on a diode-like device stored at 60°C for 236h in dark where the dark I-V became resistor-like as confirmed in Fig.S4. This is already showed from Domanski et al. stressing the device under light exposure at 75°C without sealing after 12h [55].

2.4 Light-Soaking

Light stability of the PSC is strongly dependent to the intrinsic factors (perovskite structure, the ETL and HTL layers and back-contact) and also to extrinsic ones such as environment conditions. By exploiting the sealing properties of SP-DES we are able to correlate the light-soaking stability of PSCs to the only intrinsic factors. In particular, we are able to correlate the intrinsic stability of PSCs under light-soaking stress to the dopant materials of the Spiro-OMeTAD. As already shown in literature, the oxygen doping (hereafter called O₂ Doping)[64] and cobalt-based compounds (FK102 and FK209) help to improve the charge transport properties of the Spiro-OMeTAD increasing the photovoltaic performance with respect to pristine Spiro-OMeTAD [65-67].

A set of large area PCSs are fabricated with O₂, FK102 and FK209 doping (see SI and Fig. S5 for photovoltaics performance of the cells) and stressed under light-soaking conditions at MPP. Figure 4a shows the behavior of PCE as a function of light-soaking time for a single cell of the HTM dopants batches.

By comparing the linear decrease of the PCEs extracted at MPP for each doping mechanism, the FK102 shows lower degradation rate (-0.013%/min) with respect to the PSCs with O₂ doping (-0.053%/min) and FK209 (-0.030%/min). Furthermore, we found that the transient PCE in the MPP measurement (from 0s to 10sec) is related to the hysteresis effect of the PSC in agreement with the results reported by Unger et al. [58]. This is clearly showed by the transient profile of the current densities at MPP condition (J_{MPP}) reported in Fig.4b. For each doping, the value of the hysteresis index (Tab. S2) is well correlated with the J_{MPP} decrease prior the steady-state condition. Thus, the doping mechanism in the Spiro-OMeTAD is a key point to improve the carrier extraction rate at

the perovskite/doped-Spiro-OMeTAD decreasing the hysteresis effect and enhancing the light stability [43, 68, 69].

Finally, the long-term light-soaking test is performed using FK209 as Spiro-OMeTAD dopant. The test is performed using an automated system to dynamically track the MPP under an equivalent optical incident power of 1 Sun. The white LED source permits to limit the optical excitation to the visible spectrum (450 to 750 nm) evaluating the light stability of the $\text{CH}_3\text{NH}_3\text{PbI}_3$ perovskite without considering the degradation processes induced from UV and IR components. A similar setup was also used by Burschka et al. [59] using white LED lamp and from Lejitens et al.[25] using a Xenon lamp with a 435nm-UV cut-off filter at V_{OC} bias condition.

Figure 5a reports the PCE evolution at MPP during the long-term light soaking test. The cell showed an initial PCE of 13.4% measured using class A Sun Simulator (AM1.5G, 1 Sun). The PCE rapidly decreased in the first three hours of the ageing test reaching 10.8% and then the cell recovered until PCE of 13.7%. After 40 hours, the device shows a linear PCE decrease with a slope of -0.018%/hour until the end of MPP tracking time (250 hours), corresponding to $T_{80} = 148$ hours. The same plot reports the normalized trends of J_{SC} , V_{OC} and FF acquired with an I-V scan every 20 minutes. The V_{OC} shows a shallow drop of 5% if compared to the 15% and 20% suffered by J_{SC} and FF, respectively. The picture of the aged device (Fig.5b) shows clearly the light-induced degradation of the perovskite layer around the active area. In order to investigate the origin of the light induced degradation, we conducted a combination of steady state and transient measurements before (black curves) and after (red curves) the stability test. The J-V characteristics of the stressed PSC show, beside the discussed J_{SC} reduction, a higher hysteresis with respect to the fresh cell (Fig. 5c). Moreover, the values of the dark current shows a reasonable increase for the aged device that is more evident in the low voltage range (0 to 0.6 V) where trap-assisted phenomena are generally more evident [70] (Fig.5d). This is an indication that more recombination channels of the free carriers are activated during the photo-induced degradation. To further study the relation between

light soaking and the recombination phenomena, transient photo-voltage (TPV) measurements are performed [71]. Figure 5e shows the normalized TPV decay from a steady state condition of 1 Sun to dark where the lines represent the three exponential fitting. The aged device shows a faster decay as highlighted by the reduction of one order of magnitude in the time constants (τ_3 from 10.8 to 0.9 s). Considering that the V_{OC} decay mainly results from the free-carrier recombination at Perovskite/HTL interface [72], this indicates that the visible light exposures has an evident effect on the creation of additional recombination channels as just observed in the dark J-V analysis. The figure 5f reports the TPV rise test where the V_{OC} is recorded passing through steady state dark condition to 1 Sun. The temporal profile can be associated to the efficiency in the electron transfer from the perovskite to TiO_2 (injection), and the hole transfer from the perovskite to the HTL (regeneration). The aged device shows a similar normalized trend that only differs in the fast regime (1 to 100 ms) where a slower rise profile appear. This is another indication that the hypothesized degradation of the perovskite layer can have a justification in the lower capability for the injection of the photo-generated charges. Complementary information regarding the recombination phenomena are extracted from the light intensity dependence of the V_{OC} [73]; in particular the open-circuit condition forces the photo-generated carriers to recombine within the cell. Figure 5g shows that for low level of illumination ($P_{INC} < 2 \text{ mWcm}^{-2}$) the aged device has a V_{OC} slope four times higher than the fresh device (448 and 159 mVdec^{-1}). In this regime the trap states of the TiO_2 /perovskite layer play a crucial role thanks to the lower density of charge, therefore we can argue that the light exposure improves the formation of photo-induced trapping sites in the Perovskite structure as just reported in recent works [74-76]. Further evidence is the similar slope of the V_{OC} in the intermediate and high intensity range ($P_{INC} > 2 \text{ mWcm}^{-2}$) where the high level of free-charge density suppresses the trapping and de-trapping phenomena. The same test is conducted under short circuit condition (J_{SC}) in order to highlight the charge collection under different level of illumination. The figure 5h shows similar trends of J_{SC} that were fitted by a power law respect P_{INC} . The dependence of J_{SC} with light intensity is characterized by a linear dependence ($\gamma \sim 1$) for both

fresh and aged devices with a reduction in the slope (α) from 0.2 to 0.12 AW^{-1} . This is a final indication that the photo-generated charges are not fully extracted at the contacts; we use this as a further proof of the presence of light induced trap states in the perovskite layer.

Unlike in the short time light-soaking stress [76], we do not observe a total recovering of the initial efficiency after storing the device in dark (see Fig. S7). A PCE of 11.4% (-15% with respect to initial efficiency) is measured after 14h hours storage, while after 800h in the dark the device shows a PCE of 10.2%, limiting the decrease to 24% of the initial value, thus showing the beneficial effect of the SP-DES sealing procedure. Finally, we point out that the perovskite degradation is not related to the sealing failure but it is an intrinsic effect of the light exposure. In particular, the light stress induces the migration of iodine from the MAPbI_3 perovskite leading to the formation of PbI_2 or other products as new trapping centers inside the perovskite layer[77] reducing charge collection efficiency at the MAPbI_3 /Spiro-OMeTAD interface[17].

2.5 STEM analysis

Scanning Transmission Electron Microscopy (STEM) is performed in order to investigate changes under different stress conditions on four cells sealed with the SP-D method. As shown in Figure 6, the morphology of the perovskite layer does not exhibit significant changes after 100h damp-heat, 100h thermal and 220h light soaking, confirming the results of the photovoltaic characterization. The perovskite capping layer appears quite regular and smooth in the four devices. The infiltration in the titania mesoporous layer is incomplete in some areas; we ascribe these imperfections to the up-scaling of the solvent engineering method to large area cells. Remarkably, STEM images do not show Spiro-OMeTAD degradation, sometimes visible as voids induced by air exposure[67].

3. Conclusions

To assess the stability of PSC technology it is necessary to separate the intrinsic degradation of materials and interfaces forming the cells from the one caused by the external factor such as environmental conditions, moisture etc. To this end, similarly to the approach for other thin film PV

technologies, it is necessary to develop an effective and rugged encapsulation method for perovskite solar cells and modules. The aim of this work is to develop such encapsulation strategy by testing several sealing procedures and comparing them by using accelerated life tests on encapsulated cells. Considering the importance of sealing protocols for the scaling-up of the perovskite technology, we only consider large area cells with an active area of 1.05cm^2 fabricated by solvent engineering, with an average PCE of 13.6% (batch of 23 PSCs) with a maximum PCE of 15.4%.

We find that, beside the sealing materials, the sealing procedure itself is also crucial for PSCs. In fact, thermal stress, UV curing, and high pressure, typically used in the sealing protocols, can damage the PSCs resulting in a net loss of efficiency after encapsulation. By comparing 5 different glass-glass sealing procedures we identify an optimal procedure (SP-D) based on the use of Kapton as primary sealing and glue bonded glass as secondary sealing. An additional edge sealing is used to improve the resistance to moisture (SP-DES). The optimized sealing procedure is able to maintain the initial PCE value over 1300 hours of shelf-life, while unsealed PSCs had a PCE decrease of over 20% already in the first 50 h.

The SP-DES is then exploited to assess the intrinsic stability of PSCs under different accelerated life time tests, comprising damp-heat, dry-heat and light soaking. Thanks to the edge sealing, the humidity is not affecting the integrity of the cell and the observed PCE reduction is mainly related to the temperature (40-50 °C). In fact, long time temperature stress is affecting the efficiency of PCE. We find a reduction of PCE of 0.1%/hour at 60 °C and 0.21% at 85 °C, mainly related to the degradation of Spiro-OMeTAD HTL. For both damp heat and thermal tests, there is no visible degradation of the $\text{CH}_3\text{NH}_3\text{PbI}_3$ layer, while, on the opposite, light soaking test induces visible intrinsic degradation of the $\text{CH}_3\text{NH}_3\text{PbI}_3$. A relative reduction of PCE of 0.14%/hour is found for the light-soaking test with a T_{80} (time to reduce the efficiency to 80% of the initial value) of 140 h. A thorough transient analysis of photovoltaic parameters shows an increase of photo-induced trap sites during the light soaking stress.

We point out that the proposed cost-effective sealing technique is suitable for the industrial development of perovskite-based optoelectronics devices such as solar cells, led emitting diodes and photo-detectors. It permits to evaluate the intrinsic stability of the perovskite devices with a direct correlation to constituent materials and their interfaces. Moreover, an effective sealing strategy allows a rigorous comparison of further material/fabrication improvements of perovskite technology.

Acknowledgements

F.M., L.C. and A.D.C. acknowledge funding from EU FP7 ITN “Destiny”, the European Union's Horizon 2020 framework program for research and innovation under grant agreement No. 653296 (CHEOPS) and the Italian Ministry of Economic Development in the framework of the Operating Agreement with ENEA for Research on the Electric System. G.D., S.C. and C.D. acknowledge funding from ERC under grant number 259619 76 PHOTO EM. G.D., P.A.M. and C.D. acknowledges financial support from the EU under grant number 77 312483 ESTEEM2.

Author Contributions

F.M. and A.D.C. conceived and designed the experiment. F.M. and E.L. realized the device, the sealing processes and the photovoltaic characterizations, L.C. carried out the light soaking test using automated MPPT system and the transient voltage profile measurement, G.D. and S.C. carried out the sample preparation for TEM and the microscopy characterization. All authors contributed to the discussion of the results and to the writing of the manuscript.

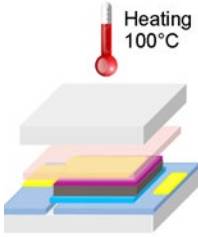
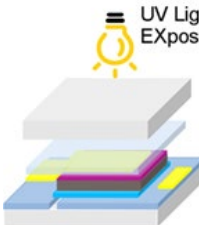
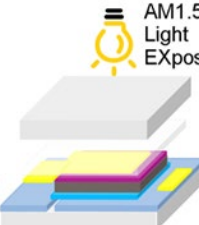
References

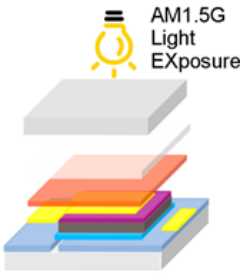
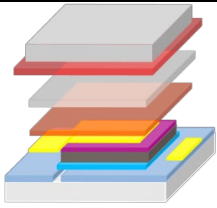
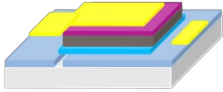
- [1] M.A. Green, K. Emery, Y. Hishikawa, W. Warta, E.D. Dunlop, Progress in Photovoltaics: Research and Applications, 23 (2015) 1-9.
- [2] R. Roesch, T. Faber, E. von Hauff, T.M. Brown, M. Lira-Cantu, H. Hoppe, Advanced Energy Materials, 5 (2015) 59-66.
- [3] http://www.nrel.gov/ncpv/images/efficiency_chart.jpg.

- [4] A. Kojima, K. Teshima, Y. Shirai, T. Miyasaka, *Journal of the American Chemical Society*, 131 (2009) 6050-6051.
- [5] J. Seo, J.H. Noh, S.I. Seok, *Accounts of Chemical Research*, 49 (2016) 562-572.
- [6] M. Gratzel, *Nat Mater*, 13 (2014) 838-842.
- [7] M.A. Green, A. Ho-Baillie, H.J. Snaith, *Nat Photon*, 8 (2014) 506-514.
- [8] Q. Chen, N. De Marco, Y. Yang, T.-B. Song, C.-C. Chen, H. Zhao, Z. Hong, H. Zhou, Y. Yang, *Nano Today*, 10 (2015) 355-396.
- [9] K. Hwang, Y.-S. Jung, Y.-J. Heo, F.H. Scholes, S.E. Watkins, J. Subbiah, D.J. Jones, D.-Y. Kim, D. Vak, *Advanced Materials*, 27 (2015) 1241-1247.
- [10] M. He, D. Zheng, M. Wang, C. Lin, Z. Lin, *Journal of Materials Chemistry A*, 2 (2014) 5994-6003.
- [11] C.R. Osterwald, T.J. McMahon, *Progress in Photovoltaics: Research and Applications*, 17 (2009) 11-33.
- [12] M.O. Reese, S.A. Gevorgyan, M. Jørgensen, E. Bundgaard, S.R. Kurtz, D.S. Ginley, D.C. Olson, M.T. Lloyd, P. Morvillo, E.A. Katz, A. Elschner, O. Haillant, T.R. Currier, V. Shrotriya, M. Hermenau, M. Riede, K. R. Kirov, G. Trimmel, T. Rath, O. Inganäs, F. Zhang, M. Andersson, K. Tvingstedt, M. Lira-Cantu, D. Laird, C. McGuinness, S. Gowrisanker, M. Pannone, M. Xiao, J. Hauch, R. Steim, D.M. DeLongchamp, R. Rösch, H. Hoppe, N. Espinosa, A. Urbina, G. Yaman-Uzunoglu, J.-B. Bonekamp, A.J.J.M. van Breemen, C. Girotto, E. Voroshazi, F.C. Krebs, *Solar Energy Materials and Solar Cells*, 95 (2011) 1253-1267.
- [13] X. Li, M. Tschumi, H. Han, S.S. Babkair, R.A. Alzubaydi, A.A. Ansari, S.S. Habib, M.K. Nazeeruddin, S.M. Zakeeruddin, M. Grätzel, *Energy Technology*, 3 (2015) 551-555.
- [14] Y. Han, S. Meyer, Y. Dkhissi, K. Weber, J.M. Pringle, U. Bach, L. Spiccia, Y.-B. Cheng, *Journal of Materials Chemistry A*, 3 (2015) 8139-8147.
- [15] J. Yang, B.D. Siempelkamp, D. Liu, T.L. Kelly, *ACS Nano*, 9 (2015) 1955-1963.
- [16] A. Mei, X. Li, L. Liu, Z. Ku, T. Liu, Y. Rong, M. Xu, M. Hu, J. Chen, Y. Yang, M. Grätzel, H. Han, *Science*, 345 (2014) 295-298.
- [17] T. Leijtens, G.E. Eperon, N.K. Noel, S.N. Habisreutinger, A. Petrozza, H.J. Snaith, *Advanced Energy Materials*, 5 (2015) 1500963.
- [18] F. Matteocci, S. Razza, F. Di Giacomo, S. Casaluci, G. Mincuzzi, T.M. Brown, A. D'Epifanio, S. Licocchia, A. Di Carlo, *Physical Chemistry Chemical Physics*, 16 (2014) 3918-3923.
- [19] T.A. Berhe, W.-N. Su, C.-H. Chen, C.-J. Pan, J.-H. Cheng, H.-M. Chen, M.-C. Tsai, L.-Y. Chen, A.A. Dubale, B.-J. Hwang, *Energy & Environmental Science*, 9 (2016) 323-356.
- [20] J.H. Noh, S.H. Im, J.H. Heo, T.N. Mandal, S.I. Seok, *Nano Lett.*, 13 (2013) 1764.
- [21] J. Zhao, B. Cai, Z. Luo, Y. Dong, Y. Zhang, H. Xu, B. Hong, Y. Yang, L. Li, W. Zhang, C. Gao, *Scientific Reports*, 6 (2016) 21976.
- [22] G. Divitini, S. Cacovich, F. Matteocci, L. Cinà, A. Di Carlo, C. Ducati, *Nature Energy*, 1 (2016) 15012.
- [23] C.C. Stoumpos, C.D. Malliakas, M.G. Kanatzidis, *Inorg. Chem.*, 52 (2013) 9019.
- [24] B. Conings, J. Drijkoningen, N. Gauquelin, A. Babayigit, J. D'Haen, L. D'Olieslaeger, A. Ethirajan, J. Verbeeck, J. Manca, E. Mosconi, F.D. Angelis, H.-G. Boyen, *Advanced Energy Materials*, 5 (2015) 1500477.
- [25] T. Leijtens, G.E. Eperon, S. Pathak, A. Abate, M.M. Lee, H.J. Snaith, *Nat Commun*, 4 (2013).
- [26] C. Law, L. Miseikis, S. Dimitrov, P. Shakya-Tuladhar, X. Li, P.R.F. Barnes, J. Durrant, B.C. O'Regan, *Advanced Materials*, 26 (2014) 6268-6273.
- [27] D. Wei, T. Wang, J. Ji, M. Li, P. Cui, Y. Li, G. Li, J.M. Mbengue, D. Song, *Journal of Materials Chemistry A*, 4 (2016) 1991-1998.
- [28] L.K. Ono, S.R. Raga, M. Remeika, A.J. Winchester, A. Gabe, Y. Qi, *Journal of Materials Chemistry A*, 3 (2015) 15451-15456.
- [29] F.K. Aldibaja, L. Badia, E. Mas-Marza, R.S. Sanchez, E.M. Barea, I. Mora-Sero, *Journal of Materials Chemistry A*, 3 (2015) 9194-9200.

- [30] I.C. Smith, E.T. Hoke, D. Solis-Ibarra, M.D. McGehee, H.I. Karunadasa, *Angewandte Chemie International Edition*, 53 (2014) 11232-11235.
- [31] R.E. Beal, D.J. Slotcavage, T. Leijtens, A.R. Bowring, R.A. Belisle, W.H. Nguyen, G.F. Burkhard, E.T. Hoke, M.D. McGehee, *The Journal of Physical Chemistry Letters*, 7 (2016) 746-751.
- [32] K.M. Boopathi, R. Mohan, T.-Y. Huang, W. Budiawan, M.-Y. Lin, C.-H. Lee, K.-C. Ho, C.-W. Chu, *Journal of Materials Chemistry A*, 4 (2016) 1591-1597.
- [33] S.N. Habisreutinger, T. Leijtens, G.E. Eperon, S.D. Stranks, R.J. Nicholas, H.J. Snaith, *Nano Lett.*, 14 (2014) 5561.
- [34] X. Li, M. Ibrahim Dar, C. Yi, J. Luo, M. Tschumi, S.M. Zakeeruddin, M.K. Nazeeruddin, H. Han, M. Grätzel, *Nat Chem*, 7 (2015) 703-711.
- [35] A. Fakharuddin, F. Di Giacomo, A.L. Palma, F. Matteocci, I. Ahmed, S. Razza, A. D'Epifanio, S. Licoccia, J. Ismail, A. Di Carlo, T.M. Brown, R. Jose, *ACS Nano*, 9 (2015) 8420-8429.
- [36] W. Chen, Y. Wu, Y. Yue, J. Liu, W. Zhang, X. Yang, H. Chen, E. Bi, I. Ashraful, M. Grätzel, L. Han, *Science*, 350 (2015) 944-948.
- [37] Y. Zhao, J. Wei, H. Li, Y. Yan, W. Zhou, D. Yu, Q. Zhao, *Nat Commun*, 7 (2016).
- [38] A. Capasso, F. Matteocci, L. Najafi, M. Prato, J. Buha, L. Cinà, V. Pellegrini, A.D. Carlo, F. Bonaccorso, *Advanced Energy Materials*, 6 (2016) 1600920.
- [39] G. Niu, W. Li, F. Meng, L. Wang, H. Dong, Y. Qiu, *Journal of Materials Chemistry A*, 2 (2014) 705-710.
- [40] S. Guarnera, A. Abate, W. Zhang, J.M. Foster, G. Richardson, A. Petrozza, H.J. Snaith, *The Journal of Physical Chemistry Letters*, 6 (2015) 432-437.
- [41] H. Si, Q. Liao, Z. Zhang, Y. Li, X. Yang, G. Zhang, Z. Kang, Y. Zhang, *Nano Energy*, 22 (2016) 223-231.
- [42] M.-C. Jung, S.R. Raga, L.K. Ono, Y. Qi, *Scientific Reports*, 5 (2015) 9863.
- [43] J.H. Kim, S.T. Williams, N. Cho, C.-C. Chueh, A.K.Y. Jen, *Advanced Energy Materials*, 5 (2015) 1401229.
- [44] Q. Tai, P. You, H. Sang, Z. Liu, C. Hu, H.L.W. Chan, F. Yan, *Nat Commun*, 7 (2016).
- [45] Y. Rong, L. Liu, A. Mei, X. Li, H. Han, *Advanced Energy Materials*, 5 (2015) 1501066.
- [46] K.D. Dobson, I. Visoly-Fisher, G. Hodes, D. Cahen, *Solar Energy Materials and Solar Cells*, 62 (2000) 295-325.
- [47] D.B. Mitzi, O. Gunawan, T.K. Todorov, K. Wang, S. Guha, *Solar Energy Materials and Solar Cells*, 95 (2011) 1421-1436.
- [48] R.J. Sutton, G.E. Eperon, L. Miranda, E.S. Parrott, B.A. Kamino, J.B. Patel, M.T. Hörantner, M.B. Johnston, A.A. Haghighirad, D.T. Moore, H.J. Snaith, *Adv. Energy Mater.*, 6 (2016) 1502458.
- [49] T. Malinauskas, D. Tomkute-Luksiene, R. Sens, M. Daskeviciene, R. Send, H. Wonneberger, V. Jankauskas, I. Bruder, V. Getautis, *ACS Applied Materials & Interfaces*, 7 (2015) 11107-11116.
- [50] W. Li, W. Zhang, S. Van Reenen, R.J. Sutton, J. Fan, A.A. Haghighirad, M.B. Johnston, L. Wang, H.J. Snaith, *Energy & Environmental Science*, 9 (2016) 490-498.
- [51] D. Bryant, N. Aristidou, S. Pont, I. Sanchez-Molina, T. Chotchunangatchaval, S. Wheeler, J.R. Durrant, S.A. Haque, *Energy & Environmental Science*, 9 (2016) 1655-1660.
- [52] E.M. Sanehira, B.J. Tremolet de Villers, P. Schulz, M.O. Reese, S. Ferrere, K. Zhu, L.Y. Lin, J.J. Berry, J.M. Luther, *ACS Energy Letters*, (2016) 38-45.
- [53] K.A. Bush, C.D. Bailie, Y. Chen, A.R. Bowring, W. Wang, W. Ma, T. Leijtens, F. Moghadam, M.D. McGehee, *Adv Mater*, 28 (2016) 3937-3943.
- [54] R.K. Misra, S. Aharon, B. Li, D. Mogilyansky, I. Visoly-Fisher, L. Etgar, E.A. Katz, *The Journal of Physical Chemistry Letters*, 6 (2015) 326-330.
- [55] K. Domanski, J.-P. Correa-Baena, N. Mine, M.K. Nazeeruddin, A. Abate, M. Saliba, W. Tress, A. Hagfeldt, M. Grätzel, *ACS Nano*, (2016) 6306-6314.
- [56] N.J. Jeon, J.H. Noh, Y.C. Kim, W.S. Yang, S. Ryu, S.I. Seok, *Nat Mater*, 13 (2014) 897-903.
- [57] H.-S. Kim, N.-G. Park, *The Journal of Physical Chemistry Letters*, 5 (2014) 2927-2934.

- [58] E.L. Unger, E.T. Hoke, C.D. Bailie, W.H. Nguyen, A.R. Bowring, T. Heumuller, M.G. Christoforo, M.D. McGehee, *Energy & Environmental Science*, 7 (2014) 3690-3698.
- [59] J. Burschka, N. Pellet, S.-J. Moon, R. Humphry-Baker, P. Gao, M.K. Nazeeruddin, M. Gratzel, *Nature*, 499 (2013) 316-319.
- [60] F.C. Krebs, T. Tromholt, M. Jorgensen, *Nanoscale*, 2 (2010) 873-886.
- [61] F. Kessler, D. Rudmann, *Solar Energy*, 77 (2004) 685-695.
- [62] S. Züfle, M.T. Neukom, S. Altazin, M. Zinggeler, M. Chrapa, T. Offermans, B. Ruhstaller, *Advanced Energy Materials*, 5 (2015) 1500835.
- [63] R. Roesch, K.-R. Eberhardt, S. Engmann, G. Gobsch, H. Hoppe, *Solar Energy Materials and Solar Cells*, 117 (2013) 59-66.
- [64] U.B. Cappel, T. Daeneke, U. Bach, *Nano Letters*, 12 (2012) 4925-4931.
- [65] J.H. Noh, N.J. Jeon, Y.C. Choi, M.K. Nazeeruddin, M. Gratzel, S.I. Seok, *Journal of Materials Chemistry A*, 1 (2013) 11842-11847.
- [66] J. Burschka, A. Dualeh, F. Kessler, E. Baranoff, N.-L. Cevey-Ha, C. Yi, M.K. Nazeeruddin, M. Grätzel, *Journal of the American Chemical Society*, 133 (2011) 18042-18045.
- [67] Z. Hawash, L.K. Ono, S.R. Raga, M.V. Lee, Y. Qi, *Chemistry of Materials*, 27 (2015) 562-569.
- [68] W. Tress, N. Marinova, T. Moehl, S.M. Zakeeruddin, M.K. Nazeeruddin, M. Gratzel, *Energy & Environmental Science*, 8 (2015) 995-1004.
- [69] V.W. Bergmann, S.A.L. Weber, F. Javier Ramos, M.K. Nazeeruddin, M. Grätzel, D. Li, A.L. Domanski, I. Lieberwirth, S. Ahmad, R. Berger, *Nat Commun*, 5 (2014).
- [70] G.-J.A.H. Wetzelaer, M. Scheepers, A.M. Sempere, C. Momblona, J. Ávila, H.J. Bolink, *Advanced Materials*, 27 (2015) 1837-1841.
- [71] P.R.F. Barnes, K. Miettunen, X. Li, A.Y. Anderson, T. Bessho, M. Gratzel, B.C. O'Regan, *Advanced Materials*, 25 (2013) 1881-1922.
- [72] V. Roiati, S. Colella, G. Lerario, L. De Marco, A. Rizzo, A. Listorti, G. Gigli, *Energy & Environmental Science*, 7 (2014) 1889-1894.
- [73] L. Gouda, R. Gottesman, A. Ginsburg, D.A. Keller, E. Haltzi, J. Hu, S. Tirosh, A.Y. Anderson, A. Zaban, P.P. Boix, *The Journal of Physical Chemistry Letters*, 6 (2015) 4640-4645.
- [74] E.T. Hoke, D.J. Slotcavage, E.R. Dohner, A.R. Bowring, H.I. Karunadasa, M.D. McGehee, *Chemical Science*, 6 (2015) 613-617.
- [75] D. Song, J. Ji, Y. Li, G. Li, M. Li, T. Wang, D. Wei, P. Cui, Y. He, J.M. Mbengue, *Applied Physics Letters*, 108 (2016) 093901.
- [76] W. Nie, J.-C. Blancon, A.J. Neukirch, K. Appavoo, H. Tsai, M. Chhowalla, M.A. Alam, M.Y. Sfeir, C. Katan, J. Even, S. Tretiak, J.J. Crochet, G. Gupta, A.D. Mohite, *Nat Commun*, 7 (2016).
- [77] F. Matsumoto, S.M. Vorpahl, J.Q. Banks, E. Sengupta, D.S. Ginger, *The Journal of Physical Chemistry C*, 119 (2015) 20810-20816.

Sealing Procedures	Sealing Materials	Curing Step	Relative PCE decrease at 20h (including encapsulation)	Relative PCE decrease at 170h
	Thermo-plastic Foil	Hot press 100°C, 0.4 bar, 40sec	-32%	-58%
SP-A				
	UV-Curable Glue	UV lamp, 40sec	-18%	-21%
SP-B				
	Light-Curable Glue	Xenon lamp, 10sec	-15%	-21%
SP-C				

	Adhesive + Light-Curable Glue	Xenon Lamp, 10sec	-4%	0%
SP-D				
	SP-D + UV- curable glue as edge sealant	SP-D + UV- cured masking the active area	0%	-2%
SP-DES				
	Unsealed	No	-7%	-33%
REF				

Tab.1. Sealing procedures (hereafter called SP-A, SP-B, SP-C, SP-D and SP-DES) for the encapsulation of the large area cells and their effect on the PCE value after 20 and 170h of shelf-life (dark, 30% relative humidity). Schematic of the sealing strategies is also reported including the conditions the cells are exposed to during the sealing procedure.

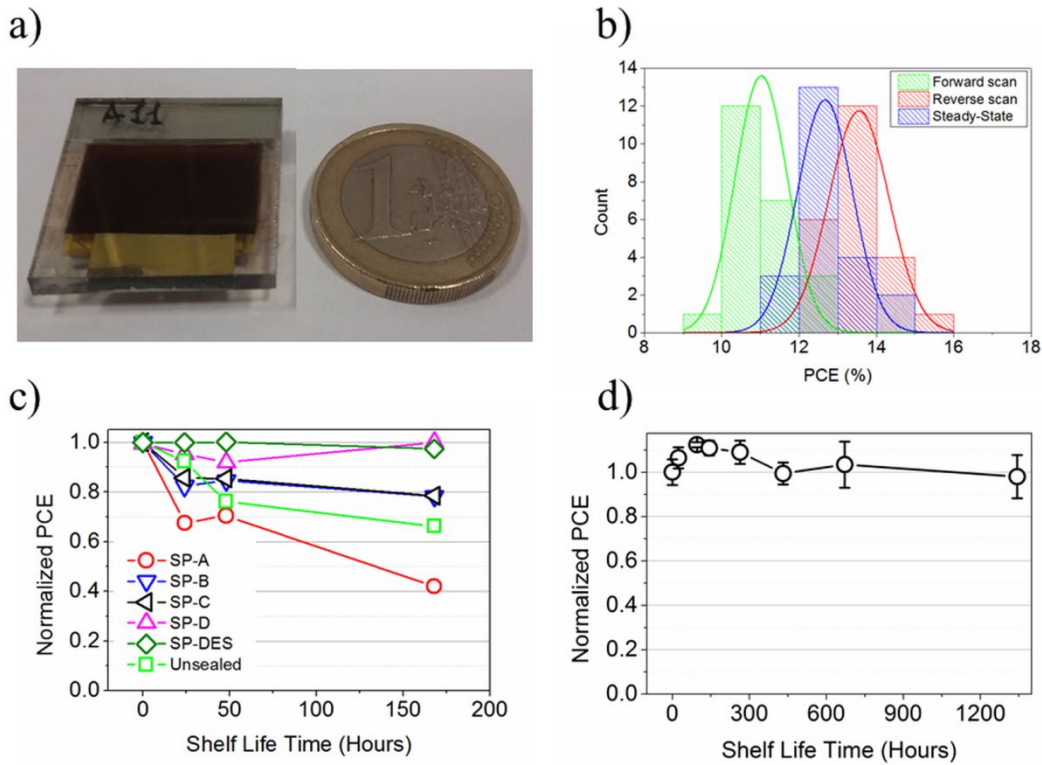


Figure 1. a) Image of large area PSC cell. b) Normal dispersions of PCE obtained measuring 23 large area cells under reverse scan (red curves), forward scan (green curves) and 180s-long MPP tracking (blue curves). c) Short-term shelf life test varying the sealing procedure. **The duration of the test was chosen in accordance with the T_{80} parameter defined in the introduction section. After 170h only SP-D and SP-DES procedures showed longer T_{80} time.** d) Long-term shelf life test (more than 1300h), using the sealing procedure SP-D. The devices were stored at low humidity (30%RH) in dark.

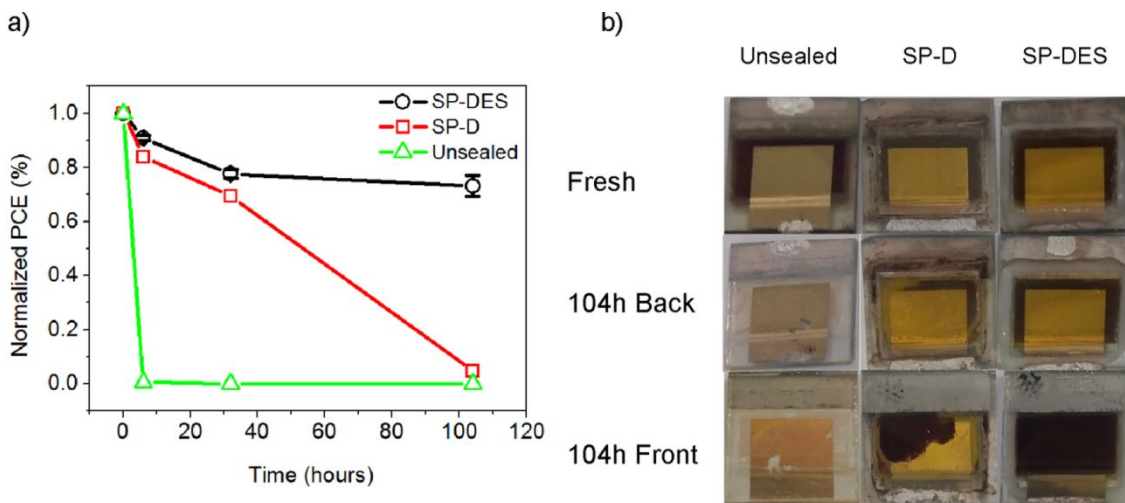


Figure 2. a) PCE behavior of the aged sealed and unsealed cells during 102h of the humidity test at 95%RH and 40-50°C temperature. b) Photographs of cells under test for different sealing procedures. The first row shows (back side) the fresh cell while second and third row show the back and front of the aged cell (104 h), respectively.

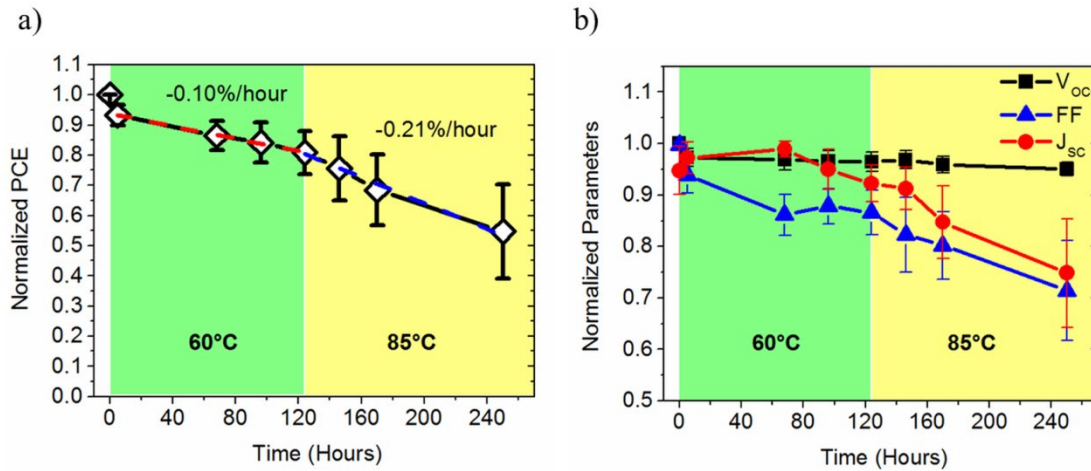


Figure 3. Evolution of the normalized photovoltaic parameters under thermal stress in an oven for 250 hours. The temperature is 60°C for the first 124 hours and then set to 85°C between 124 hours and 250 hours. a) Normalized PCE. Linear fittings are reported for both temperatures: 60°C (red line) and 85°C (blue line). b) V_{OC} (black squares), J_{sc} (red circles), Fill Factor (circles).

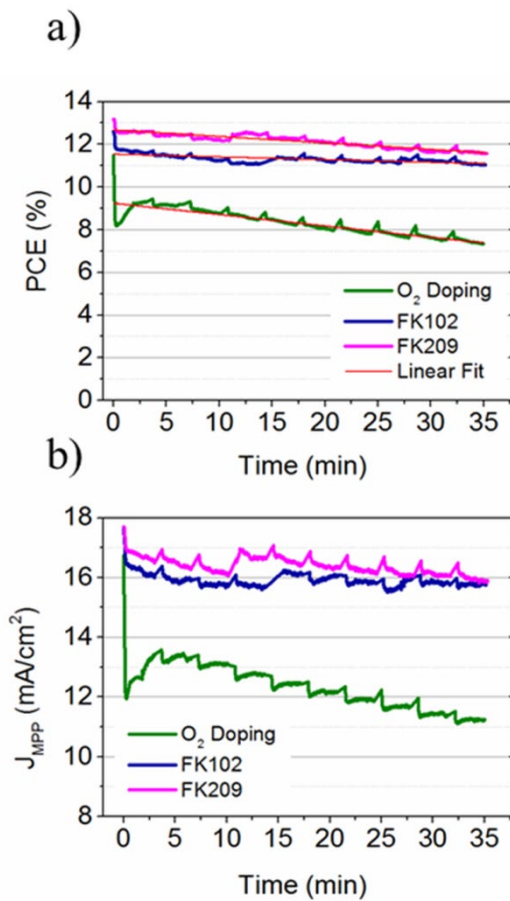


Figure 4.a) I-V characteristics of sealed cell varying the p-doping method (O₂ doping, blue curve; FK102, green curve and FK209, red curve) realized before the short-term light soaking test. b) The PCE results were reported during Short-term light soaking test (35minutes) at MPP for each doping-method. The I-V characteristic were measured every 3 minutes under forward scan direction (10mV as step voltage).

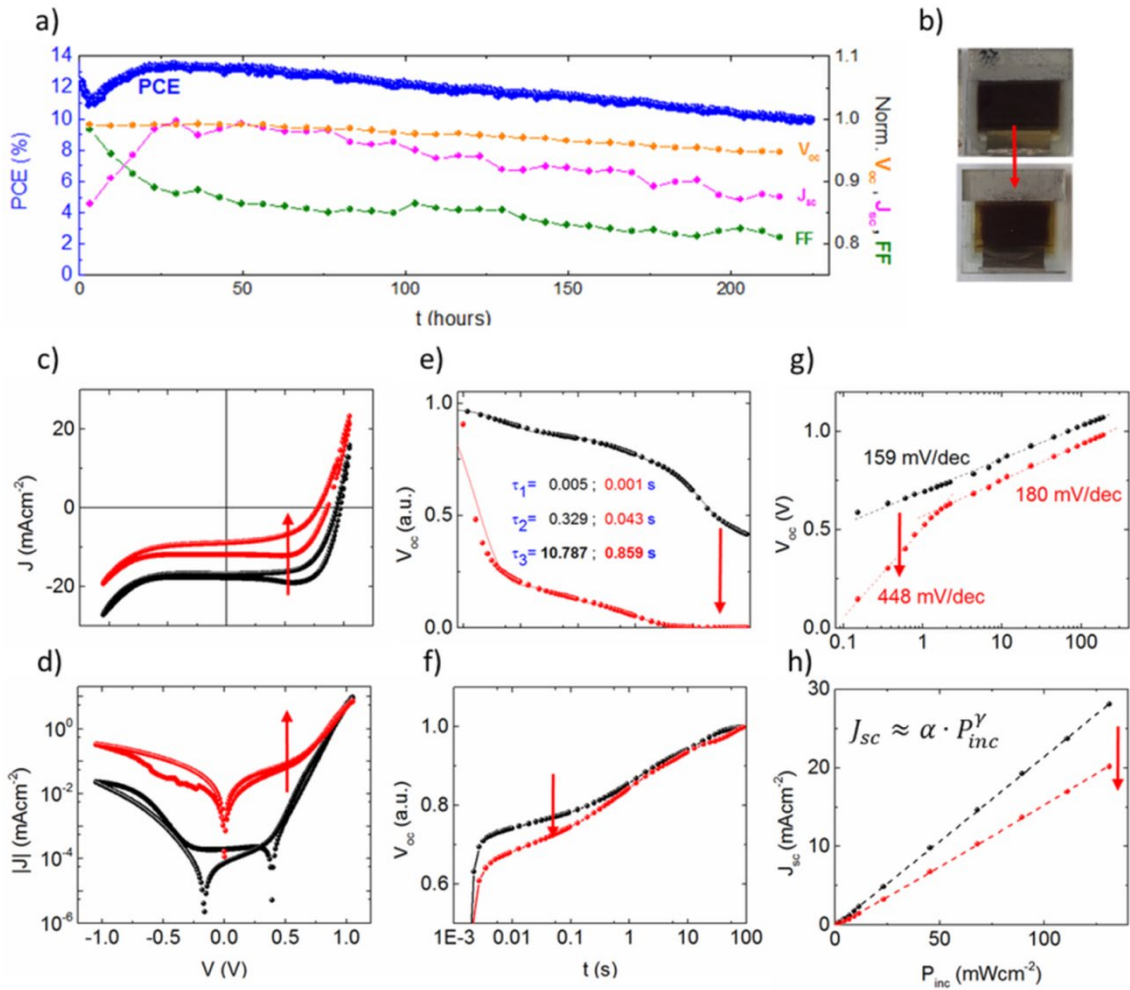


Figure 5. a) Temporal trend of the PCE over the 250 hours of stability test with MPP tracking; the right axes reports the V_{OC} , J_{SC} and FF extracted every 20 minutes by a J-V scan. b) The optical images of the active area before and after the stability test; c) Forward and reverse scan of J-V curves before (black) and after (red); d) the J-V under dark condition on a semi-log plot; e) Transient Photo-Voltage (TPV) decay test from 1 Sun to dark condition; the line represents the fitting with a three-exponential function, the extracted time constants are reported. f) TPV rise test from dark to 1 Sun condition, g) V_{OC} versus the optical incident power (P_{INC}) from 0.001 to 1.5 Sun; the dashed lines are the logarithmic fitting. h) J_{SC} versus the optical incident power (P_{INC}) from 0.001 to 1.5 Sun where the dashed lines are the power law fittings.

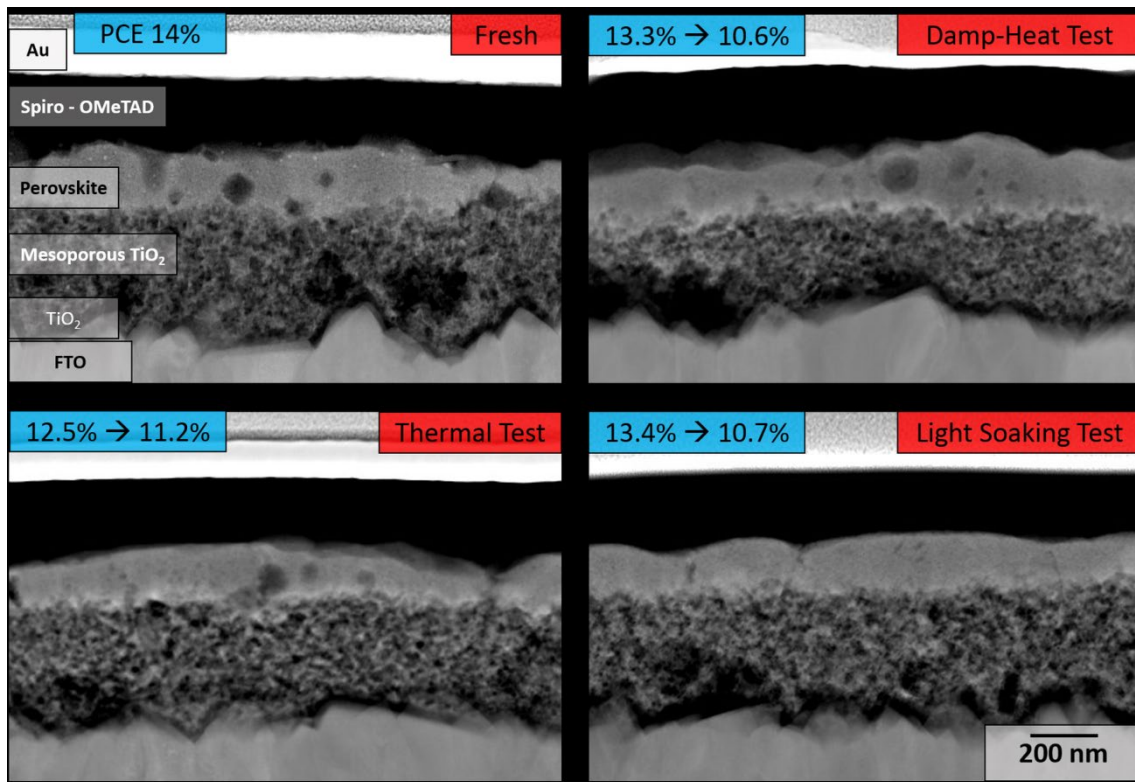


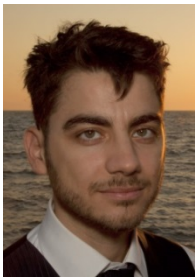
Figure 6. High angle annular dark field scanning transmission electron microscopy (HAADF STEM) images of a fresh cell (a) and cells sealed employing the SP-D method after 100 h damp heat (b), 100 h thermal (c) and 220 h light (d) exposure. Scale bar applies to all images. The blue labels report PCE values for the 4 devices before and after stress tests.

Vitae



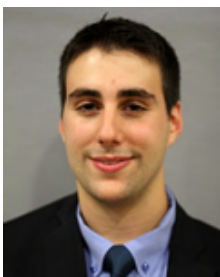
Fabio Matteocci was born in Rome, (Italy) in 1983. He received the Degree in Electronic Engineering from the University of Rome “Tor Vergata” (Italy) in 2009 and his Ph.D. degree in electrical engineering from the Center for Hybrid and Organic Solar Energy (CHOSE) in 2014. He is a researcher at CHOSE lab.

He is mainly working on the development of scalable realization processes for thin-film photovoltaic technologies such as solid-state DSCs and perovskite solar cell.



Lucio Cinà received the M.Sc. degree summa cum laude in Electronic Engineering at University of Rome “Tor Vergata” (Italy) in 2009 and his Ph.D. degree from the Center for Hybrid and Organic Solar Energy (CHOSE) of Lazio region in 2013. He is currently post-doc researcher of Prof. Aldo Di Carlo group

(CHOSE). His research activity concerns the development of advanced electro-optical characterization systems for hybrid photovoltaic devices. He also deals with degradation process test by using electrochemical impedance analysis and improved-LBIC mapping, in particular Perovskite based Solar Cells (PSC).



Enrico Lamanna received his M.S. degree in Electronic Engineering from the University Rome of Tor Vergata. He is now a candidate to become Ph.D. student in Electronic Engineering at the University of Rome Tor Vergata (Centre for Hybrid and Organic Solar Energy – CHOSE). His research interests currently

include the development of perovskite solar cells, with focus on silicon/perovskite tandem devices.



Stefania Cacovich is currently a PhD student of the Electron Microscopy group in the department of Materials Science and Metallurgy, University of Cambridge, working under the supervision of Dr Cate Ducati. She obtained a BSC and MSC in Materials and Chemical Engineering from the University of

Trieste, Italy. Her research focuses on the application of the latest developments in analytical TEMs and data processing for the characterisation of nanostructured composites for energy application, in particular hybrid perovskites for photovoltaic devices.



Giorgio Divitini obtained his Bachelor's and Master's degrees in Physics from the University of Milan, Italy, before receiving a PhD in Materials Science from the University of Cambridge, UK. He is currently a post-doctoral research associate at the University of Cambridge, working on electron microscopy for

the characterisation of nanostructured materials and devices.



Paul Midgley is Professor of Materials Science and Director of the Electron Microscopy Facility. He is a Fellow of the Royal Society and a Professorial Fellow at Peterhouse. Before moving to Cambridge in 1997, he held two Research Fellowships in the H.H. Wills Physics Laboratory at the University of

Bristol, He has studied a wide variety of materials by electron microscopy and developed a number of novel electron microscopy techniques. His recent research has concentrated on electron tomography, electron holography, energy filtered TEM and precession electron diffraction.



Caterina Ducati is a Reader in Nanomaterials and part of the Electron Microscopy group in Cambridge. She graduated in Physics in Milan in 1999, and received her PhD in Engineering from Cambridge in 2003. After a postdoc under the supervision of Prof Paul Midgley, she was awarded a Dorothy Hodgkin Fellowship in 2004, and a Royal Society University Research Fellowship in 2007. She was appointed to a Lectureship in Materials Science in 2009. She is interested in energy materials, and in particular photoactive nanostructured compounds for applications in photovoltaics and photocatalysis, but also in novel nanomaterials for electrochemical cells.



Aldo Di Carlo received his degree in Physics (with honors) from the University of Rome "La Sapienza" (Italy) in 1991 and his Ph.D. degree from the Technische Universität München (Germany) in 1995. He is currently a Full Professor of Optoelectronics and Nanoelectronics at the University of Rome "Tor Vergata" (Italy), and since 2006, he has also been co-director of the Centre for Hybrid and Organic Solar Energy (CHOSE). His research activity mainly concerns the study of electronic transport and optoelectronic properties of nanostructured and organic semiconductor devices and their fabrication.